

# The structure of the phenol-nitrogen cluster: A joint experimental and *ab initio* study

Michael Schmitt<sup>a)</sup> and Christian Ratzer

Heinrich-Heine-Universität, Institut für Physikalische Chemie, D-40225 Düsseldorf, Germany

W. Leo Meerts<sup>b)</sup>

Department of Molecular and Laser Physics, University of Nijmegen, NL-6500 GL Nijmegen, The Netherlands

(Received 26 September 2003; accepted 12 November 2003)

The rotationally resolved LIF spectra of four different isotopomers of the phenol-nitrogen cluster have been measured to elucidate the structural parameters of the cluster in ground and electronically excited ( $S_1$ ) state. The fit of the rotational constants has been performed by a genetic algorithm and by an assigned fit to the line frequencies. The results of both methods are compared. The intermolecular structures are fit to the inertial parameters and are compared to the results of *ab initio* calculations for both states. This fit was performed under the restriction that the geometry of the monomer moieties do not change upon complexation. Of the remaining five intermolecular parameters two dihedral angles were fixed due to the planarity of the complex, which was inferred from the inertial defects of all isotopomers. The distance of the nearest nitrogen atom to the hydrogen atom of the phenolic hydroxy group is found to decrease upon electronic excitation of the chromophore considerably more than predicted from *ab initio* calculations. This deviation between theory and experiment can be traced back to the absence of electron–electron correlation in the performed complete active space self-consistent field calculations. The shortening of the OH $\cdots$ NN “hydrogen” bond upon electronic excitation is in agreement with the increased dipole moment of phenol in the  $S_1$ -state. © 2004 American Institute of Physics. [DOI: 10.1063/1.1638378]

## I. INTRODUCTION

van der Waals clusters between aromatic molecules and noble gas atoms have been investigated in the past in great detail. In all cases the noble gas is found to be situated above the aromatic ring ( $\pi$ -bond) with typical distances of about 350 pm for Ar and 340 pm for Ne atoms.

For three monohalobenzenes (F,Cl,Br) the complexes with nitrogen were also determined to be van der Waals bound<sup>1</sup> above the aromatic ring. The aniline-nitrogen system has been studied using rotationally resolved electronic spectroscopy and was found to be van der Waals bound with a perpendicular distance of the nitrogen molecule from the aromatic plane of 343.3 pm.<sup>2</sup>

For the nitrogen-phenol cluster one would expect a bonding similar to the van der Waals clusters from the previous paragraph. However it was shown by the group of Müller–Dethlefs that the structure of phenol-N<sub>2</sub> in the ground state, in the electronically excited state, and in the cation is dominated by dipole–quadrupole interactions. This leads to a “hydrogen bond” type of geometry, rather than electron dispersion interactions, that favor the van der Waals geometry.<sup>3–5</sup> The structure of phenol-nitrogen in the electronic ground state was extracted by Müller–Dethlefs from a rotational band contour analysis of the REMPI spectrum of the electronic origin of the complex.<sup>5</sup> Fuji *et al.*<sup>6</sup> studied the ground state of the complex using IR-UV double resonance

spectroscopy and found a slight redshift of  $-5\text{ cm}^{-1}$  of the intramolecular OH-stretching vibration, with respect to the value in the monomer, while in the  $D_0$ -state a redshift of  $-159\text{ cm}^{-1}$  was found. The redshift of the OH-stretching vibration is considerably smaller than in “real” hydrogen bond systems like phenol-water with  $-133\text{ cm}^{-1}$ .<sup>7,8</sup>

Watkins *et al.*<sup>9</sup> performed complete active space self-consistent field (CASSCF) calculations with an active space of eight electrons in seven orbitals, including exclusively  $\pi$ -type orbitals from phenol. These calculations give a prediction of the structure of the phenol-nitrogen complex in the  $S_0$  and the  $S_1$ -state.

Solca and Dopfer<sup>10</sup> investigated the phenol-N<sub>2</sub> cation using IR spectroscopy and found a proton bound species for this cluster.

In this paper we present the first high resolution study of the electronic origins of four isotopomers of the phenol-nitrogen cluster: phenol-N<sub>2</sub>,  $d_1$ -phenol-N<sub>2</sub>,  $d_5$ -phenol-N<sub>2</sub>, and  $d_6$ -phenol-N<sub>2</sub>. These data allow a unique structure determination of this complex. This structure will be compared to the results of *ab initio* calculations. Furthermore we determined the  $S_1$ -state lifetimes of all isotopomers from a rovibronic band contour analysis of all isotopomers used in this study.

## II. EXPERIMENT

The experimental setup for the rotationally resolved LIF is described elsewhere.<sup>11</sup> Briefly, it consists of a ring dye laser (Coherent 899-21) operated with Rhodamine 110,

<sup>a)</sup>Electronic mail: mschmitt@uni-duesseldorf.de

<sup>b)</sup>Electronic mail: Leo.Meerts@sci.kun.nl

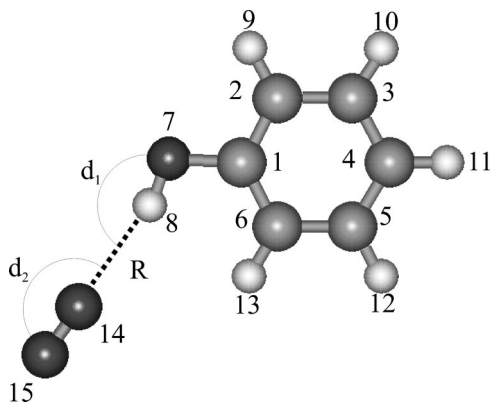


FIG. 1. Atomic numbering and definitions of the geometry parameters used in the fit.

pumped with 6 W of the 514 nm line of an Ar<sup>+</sup>-ion laser. The light is coupled into an external folded ring cavity<sup>12</sup> for the second harmonic generation (SHG). The molecular beam is formed by expanding phenol, seeded in 400 mbar of a mixture of argon and nitrogen (80:20), through a 70  $\mu$ m hole into the vacuum. The molecular beam machine consists of three differentially pumped vacuum chambers that are linearly connected by skimmers (1 mm and 3 mm, respectively) in order to reduce the Doppler width. The molecular beam is crossed at right angles in the third chamber with the laser beam 360 mm downstream of the nozzle. The resulting fluorescence is collected perpendicular to the plane defined by laser and molecular beam by an imaging optics setup consisting of a concave mirror and two plano-convex lenses. The resulting Doppler width in this set-up is 25 MHz (FWHM). The integrated molecular fluorescence is detected by a photomultiplier tube whose output is discriminated and digitized by a photon counter and transmitted to a PC for data recording and processing. The relative frequency is determined with a quasi confocal Fabry–Perot interferometer with a free spectral range (FSR) of 149.9434(56) MHz. The FSR has been calibrated using the combination differences of 111 transitions of indole for which the microwave transitions are known.<sup>13,14</sup> The absolute frequency was determined by recording the iodine absorption spectrum and comparing the transitions to the tabulated lines.<sup>15</sup>

### III. RESULTS

We used four different isotopomers in this study. They will be defined in the following. In phenol-N<sub>2</sub> all elements are contained as the most abundant isotopomeric species (<sup>12</sup>C, <sup>1</sup>H, <sup>16</sup>O, <sup>14</sup>N). In  $d_1$ -phenol-N<sub>2</sub> the hydrogen atom of the hydroxy group of phenol (position 8 in Fig. 1) is replaced by deuterium.  $d_5$ -phenol-N<sub>2</sub> means complete ring deuteration (positions 9–13 in Fig. 1) and  $d_6$ -phenol-N<sub>2</sub> represents the completely ring and hydroxy deuterated isotopomer (positions 8–13 in Fig. 1).

The rotationally resolved electronic spectrum of the electronic origin of phenol-N<sub>2</sub> is shown in trace (a) of Fig. 2. The origin band is an  $a/b$ -hybrid band due to reorientation of the inertial axes in the cluster with respect to the monomer axes. In the monomer the orientation of the transition dipole

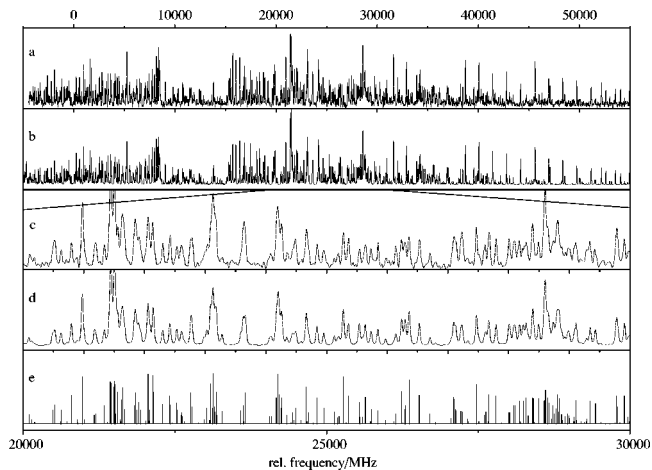


FIG. 2. (a) Rotationally resolved electronic spectrum of the electronic origin of phenol-N<sub>2</sub>. (b) Simulation, using the inertial parameters, given in Table III. (c) Expanded view of trace (a). (d) Simulation in the same spectral range with Voigt convoluted line shapes, using a Gaussian width of 26 MHz and a Lorentzian width of 39.4 MHz. (e) Stick spectrum in the same spectral range.

is almost exactly along its inertial  $b$ -axis. The observed spectrum consists of about 400 clusters of lines, with only a few single rovibronic lines [cf. the expanded view of the spectrum in trace (c) with the simulated stick spectrum shown in trace (e) of Fig. 2]. This massive overlap is due to the relatively small rotational constants of the complex. For this reason a fit of the spectrum using the quantum number assigned line positions to an appropriate Hamiltonian is very difficult. A problem like this, which arises frequently in congested spectra, can be solved with the aid of a fit based on a genetic algorithm (GA). In such a fit the contour and shape of the spectrum is used and it does not rely on the assignments of individual rovibronic lines. The fitting procedure using GA has been described in detail elsewhere.<sup>16,17</sup>

The initial search range for the parameters in the GA fit was obtained from a preliminary *ab initio* calculation. This calculation was based on a “hydrogen bonded” structure as proposed by Ford *et al.*<sup>5</sup> With the limits of the parameters given in Table I, the GA converged very rapidly. A visual inspection on the final simulation showed a perfect match with the experimental spectrum. The molecular parameters obtained from the GA fit are presented in the second column of Table II. The values given and the quoted uncertainties are the result of a statistics on ten independent GA runs, with different initial seeds, i.e., different starting populations of the evolution.

In a second step, we used the results of the GA calculation to assign quantum numbers to the individual transitions and cluster of lines. Because of the high quality of the GA fit, this was an easy task in spite of the large number of overlapping lines. With these line positions assignments a second fit to the parameters of a rigid rotor Hamiltonian for both electronic states is performed that in particular yields better values for the uncertainties of the parameters. For most parameters the values obtained from the line fit (Table II, column 1) agree within their uncertainties to the corresponding GA results.

TABLE I. Input parameters and limits for the genetic algorithm fit of the spectrum of the phenol-nitrogen complex.  $\Delta A$  is defined as the difference of ground state and excited state rotational  $A$  constant  $A'' - A'$ , etc.

	Lower	Upper	Guess
$A''/\text{MHz}$	4000	4100	4034
$B''/\text{MHz}$	600	650	635
$C''/\text{MHz}$	520	570	548
$\nu_0/\text{MHz}^a$	13500	15500	14500
$T/\text{K}$	1	5	3
$\theta/^\circ$ <sup>b</sup>	50	70	60
$\Delta A'/\text{MHz}$	-150	-50	-100
$\Delta B'/\text{MHz}$	0	20	11
$\Delta C'/\text{MHz}$	0	20	6
$\Delta_{\text{Gauss}}/\text{MHz}^c$			25
$\Delta_{\text{Lorentz}}/\text{MHz}$	10	40	18

<sup>a</sup>The band origin is given in MHz relative to the start of the scan.

<sup>b</sup>The angle  $\theta$  is defined as angle between the transition dipole moment and the inertial  $a$ -axis.

<sup>c</sup>The Gaussian width was kept fix at the experimentally determined Doppler width of 25 MHz.

The spectra of the other three isotopomers ( $d_1$ -phenol- $\text{N}_2$ ,  $d_5$ -phenol- $\text{N}_2$ , and  $d_6$ -phenol- $\text{N}_2$ ), shown in Fig. 3 have been treated in the same way. A compilation of the final molecular parameters is given in Table III. All isotopomers are near prolate asymmetric rotors, with a small negative inertial defect in both electronic states, indicating the planarity of the complex in both electronic states.

The shifts of the electronic origins with respect to the origin of phenol- $\text{N}_2$  are also given in Table III. These isotopic shifts are due to different zero-point energies of the isotopomers in both electronic states and are very similar to the respective shifts of the phenol monomer.

Since the GA performs a line shape fit of the complete spectrum, much better information on the linewidth is gathered than from a line shape fit to a few individual lines. In order to obtain the relevant parameters that determine the intensities in the spectrum, we performed a second GA fit with a reduced search range and a weight function width<sup>16</sup> narrowed down to zero. This resulted in improved values for the angle  $\theta$  ( $\cos \theta = \mu_a/\mu_b$ ) and the Lorentzian component of the linewidth. The Gaussian width is fixed to the experimentally determined value of 25 MHz. The temperature depen-

TABLE II. Comparison of the molecular parameters of the phenol-nitrogen cluster as obtained from an assigned fit and from the genetic algorithm fit.  $S$  is the standard deviation of the fit.

	Assigned	GA-fit
$A''/\text{MHz}$	4072.18(25)	4071.06(13)
$B''/\text{MHz}$	648.01(4)	647.89(2)
$C''/\text{MHz}$	559.26(4)	559.13(2)
$\Delta I''/\text{u}\text{\AA}^2$	-0.354(43)	-0.369
$\Delta A/\text{MHz}$	-141.560(91)	-140.99(6)
$\Delta B/\text{MHz}$	15.708(13)	15.71(1)
$\Delta C/\text{MHz}$	8.671(9)	8.70(1)
$\Delta I'/\text{u}\text{\AA}^2$	-0.162(50)	-0.188
$\nu_0/\text{MHz}$	14594.0(7)	14593.23(45)
Number of lines	118	1990
$S/\text{MHz}$	3.72	...

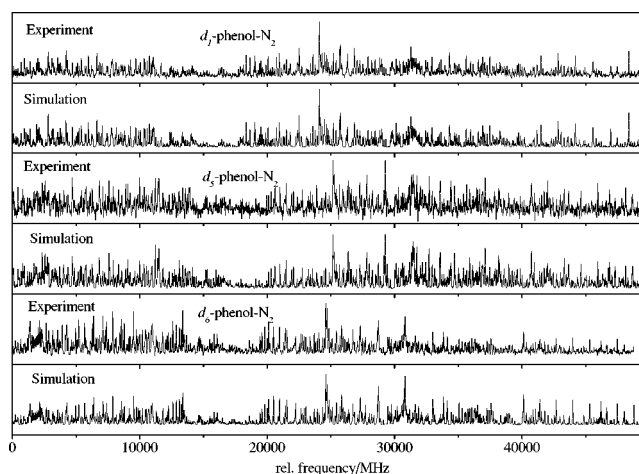


FIG. 3. Rotationally resolved electronic spectrum of the electronic origins of  $d_1$ -,  $d_5$ -, and  $d_6$ -phenol- $\text{N}_2$  along with the simulation, using the inertial parameters, given in Table III.

dence of the intensity is described by a two temperature model,<sup>18</sup>

$$n(T_1, T_2, w) = e^{-E/kT_1} + w e^{-E/kT_2}, \quad (1)$$

where  $E$  is the energy of the lower state,  $k$  is the Boltzmann constant,  $w$  is a weighting factor,  $T_1$  and  $T_2$  are the two temperatures. The resulting temperatures and weights obtained from the individual spectra of the four isotopomers are presented in Table IV.

#### A. Lifetimes

The Lorentzian linewidths (and therefore the  $S_1$ -state lifetimes) show a characteristic pattern which depends more or less only on the isotopic substitution at the phenolic hydroxy group. The pattern is similar to that found for the phenol monomer. Isotopic substitution of H with D at the phenolic hydroxy group leads to a reduction of Lorentzian width and thus to a longer  $S_1$ -state lifetime. While complexation of phenol with water increases the lifetime from 2 ns to 15 ns, the lifetime of the complex with nitrogen is found to be 8 ns. Phenol-water and  $d_1$ -phenol-water have the same lifetime of 15 ns, while for phenol-nitrogen the lifetime increases upon isotopic substitution of hydrogen with deuterium at the phenolic hydroxy group (see Table IV).

Sobolewski and Domcke<sup>19</sup> discussed a conical intersection of the repulsive  $^1\pi\sigma^*$  potential energy surface with the originally excited  $^1\pi\pi^*$  surface and a subsequent intersection with the ground state potential energy surface to account for the short lifetime of phenol. The longer lifetimes of the deuterated phenol and the phenol-water clusters are attributed to different mechanisms. In the first case, the probability of tunneling through the barrier which separates the  $^1\pi\sigma^*$  from the  $^1\pi\pi^*$  surface is reduced due the smaller zero-point energy of the deuterated phenol. In the latter, the form of the electronic potential functions is changed, so that the intersection of the  $^1\pi\sigma^*$  with the ground state is removed. This leads to the observed increase of the lifetime in the phenol-water cluster.

Another explanation for the increasing lifetime of the deuterated phenol as well as of the water cluster was pre-

TABLE III. Molecular constants of phenol-N<sub>2</sub>, [7D]phenol-N<sub>2</sub>, *d*<sub>5</sub>-phenol-N<sub>2</sub>, and *d*<sub>6</sub>-phenol-N<sub>2</sub> obtained from assigned fits of the line positions to a rigid rotor Hamiltonian. For details see text. *S* is the standard deviation of the fit.

	phenol-N <sub>2</sub>	<i>d</i> <sub>1</sub> -phenol-N <sub>2</sub>	<i>d</i> <sub>5</sub> -phenol-N <sub>2</sub>	<i>d</i> <sub>6</sub> -phenol-N <sub>2</sub>
<i>A</i> <sup>o</sup> /MHz	4072.18(25)	4050.44(24)	3567.71(19)	3548.50(32)
<i>B</i> <sup>o</sup> /MHz	648.01(4)	647.88(4)	622.41(3)	621.79(6)
<i>C</i> <sup>o</sup> /MHz	559.26(4)	558.71(3)	530.229(23)	529.28(5)
$\Delta I^o/\text{u}\text{\AA}^2$	-0.354(43)	-0.269(49)	-0.492(36)	-0.362(59)
$\Delta A/\text{MHz}$	-141.560(91)	-140.41(10)	-116.64(7)	-116.31(12)
$\Delta B/\text{MHz}$	15.708(13)	15.42(2)	14.51(1)	14.27(2)
$\Delta C/\text{MHz}$	8.671(9)	8.51(1)	7.653(6)	7.42(1)
$\Delta I^o/\text{u}\text{\AA}^2$	-0.162(50)	-0.183(80)	-0.342(55)	-0.152(104)
$\tilde{\nu}_0/\text{cm}^{-1}$	36249.16	36246.62	36419.62	36416.98
$\Delta\tilde{\nu}_0/\text{cm}^{-1}$	0	-2.54	170.46	167.82
Number of lines	118	119	139	83
<i>S</i> /MHz	3.72	3.90	4.48	4.78

sented by Lipert *et al.*<sup>20</sup> The short excited state lifetime of phenol was attributed to a rapid internal conversion (IC), with the ground state OH stretching vibration as a promoter mode.<sup>20,21</sup> The frequency of this promoter mode shifts to lower frequencies upon deuteration as well upon cluster formation, which is believed to cause the increase in lifetime. For the phenol-water cluster a redshift of  $-133\text{ cm}^{-1}$  of the OH-stretching vibration is found,<sup>7,8</sup> while for phenol-nitrogen the experimentally determined redshift is only  $-5\text{ cm}^{-1}$ .<sup>6</sup> Such a small shift of the frequency of the promoter mode cannot account for the large change in lifetime observed in the experiment.

A decision, which of both models applies, has to be postponed until a CASPT2 profile for ground state,  $^1\pi\sigma^*$ , and  $^1\pi\pi^*$  state along the OH-stretch coordinate is calculated. This work is under way.

## B. Determination of the structure

The program PKRFIT (Ref. 22) was used to determine the structure of the phenol-N<sub>2</sub> cluster in the *S*<sub>0</sub> and *S*<sub>1</sub>-states. Figure 1 shows the atomic numbering and the definitions of the geometrical parameters. The structure given in Fig. 1 represents just one input geometry for the fit. As the Levenberg–Marquardt fitting algorithm<sup>23,24</sup> that was used for the geometry fitting is a local optimizer we tested several other starting geometries. They had either a higher value of the cost function or converged to the same minimum. The rotational constants of the four isotopomers discussed in the previous section were used as input. The monomer geometry of phenol in the *S*<sub>0</sub>-state has been kept fixed to the

*r*<sub>*s*</sub>-structure, obtained by Larsen via microwave spectroscopy,<sup>25</sup> the *S*<sub>1</sub>-geometry parameters for phenol are taken from Ref. 22. The N–N distance in the nitrogen molecule has been kept fixed to a value of 109.77 pm as determined by Berndtsen<sup>26</sup> using Raman spectroscopy. Therefore the only geometry parameters to be determined are the five intermolecular degrees of freedom between the phenol and nitrogen constituents. From the small negative inertial defect of all isotopomers (Table III) we can immediately conclude that the complex is planar in both the *S*<sub>0</sub> and *S*<sub>1</sub>-state. Consequently, the two dihedral angles were set to 0°. The remaining three geometrical parameters were fitted to the rotational constants of the four phenol-nitrogen isotopomers. We performed two different structural fits: one to the *r*<sub>0</sub>-structure, which completely neglects the different vibrational contributions from the different isotopomers and is based on the following assumption:

$$I_0^g = I_{\text{rigid}}^g(r_0). \quad (2)$$

The second is a fit to the pseudo-*r*<sub>*s*</sub>-structure. The latter takes into account the vibrational effects of the different isotopomers via three parameters  $\epsilon_{0g}$  that describe the average vibrational contributions with respect to the inertial axes *g*,<sup>27</sup>

$$I_0^g = I_{\text{rigid}}^g(r_s) + \frac{1}{2}\epsilon_{0g}. \quad (3)$$

In these equations *I*<sub>0</sub><sup>*g*</sup> are the (experimentally determined) zero-point averaged moments of inertia with respect to the inertial axes *g*. The functions *I*<sub>rigid</sub><sup>*g*</sup>(*r*<sub>0</sub>) or *I*<sub>rigid</sub><sup>*g*</sup>(*r*<sub>*s*</sub>) are calculated from the structural parameters *r*<sub>0</sub> or *r*<sub>*s*</sub>, respectively, using rigid-molecule formulas. The  $\epsilon_{0g}$  are the vibrational corrections, which are assumed to be the same for all isotopomers. The inertial parameters, which are calculated from Eqs. (2) and (3), are compared to the experimental rotational constants in Table V. The difference between a fit to the pseudo-*r*<sub>*s*</sub>-structure and the *r*<sub>0</sub>-structure is small. Regarding the weak intermolecular bond, that gives rise to very low frequency vibrations with large amplitudes, this finding is somehow surprising.

The resulting geometrical parameters for the ground and electronically excited states are presented in Table VI. The *r*<sub>0</sub>-distance between the hydrogen atom of the hydroxy group and the closest nitrogen atom in the electronic ground state is

TABLE IV. Parameters that determine the relative intensities in the spectra of phenol-N<sub>2</sub>, [7D]phenol-N<sub>2</sub>, *d*<sub>5</sub>-phenol-N<sub>2</sub>, and *d*<sub>6</sub>-phenol-N<sub>2</sub> obtained from a GA fit. For details see text.

	phenol-N <sub>2</sub>	<i>d</i> <sub>1</sub> -phenol-N <sub>2</sub>	<i>d</i> <sub>5</sub> -phenol-N <sub>2</sub>	<i>d</i> <sub>6</sub> -phenol-N <sub>2</sub>
<i>T</i> <sub>1</sub> /K	4.03(26)	1.63(22)	3.13(41)	3.59(18)
<i>T</i> <sub>2</sub> /K	1.54(43)	2.23(33)	3.87(50)	0.47(21)
<i>w</i>	0.42(8)	0.68(4)	0.42(14)	0.78(9)
$\theta^\circ$	59.87(4)	62.53(7)	59.14(7)	60.05(1)
$\Delta_{\text{Lorentz}}/\text{MHz}$	39.4(2)	18.7(1)	39.8(6)	23.2(3)
$\tau/\text{ns}$	8.1(1)	17.0(1)	8.0(2)	13.7(2)



TABLE V. Experimentally determined and fitted rotational constants of the electronic ground state of phenol-N<sub>2</sub>, using the model given in Fig. 1.

	Experiment	Calculated pseudo- $r_s$	Difference	Calculated $r_0$	Difference
phenol-N <sub>2</sub>					
A"/MHz	4072.180	4068.056	4.124	4068.402	3.778
B"/MHz	648.010	648.963	-0.953	649.335	-1.325
C"/MHz	559.260	559.912	-0.652	559.963	-0.703
$d_1$ -phenol-N <sub>2</sub>					
A"/MHz	4050.445	4050.789	-0.344	4050.621	-0.176
B"/MHz	647.885	647.144	0.741	647.563	0.322
C"/MHz	558.710	558.231	0.479	558.307	0.403
$d_5$ -phenol-N <sub>2</sub>					
A"/MHz	3567.704	3568.402	-0.698	3568.929	-1.225
B"/MHz	622.410	622.615	-0.205	622.714	-0.304
C"/MHz	530.229	530.330	-0.099	530.203	0.026
$d_6$ -phenol-N <sub>2</sub>					
A"/MHz	3548.500	3554.580	-6.080	3554.697	-6.197
B"/MHz	621.796	620.752	1.043	620.896	0.900
C"/MHz	529.286	528.673	0.613	528.571	0.715

233.1(3) pm. This bond distance decreases to 220.8(21) pm upon electronic excitation. The corresponding values for the pseudo- $r_s$ -structure are 225.5(13) and 211.0(6) pm. For both geometries a very similar decrease in bond length upon electronic excitation has been found. Along with the shortening of the "hydrogen bond," the N-N··H angle gets more linear in the  $S_1$ -state. The pseudo- $r_s$ -structures of both electronic states are shown in Fig. 4.

### C. Comparison to the results of *ab initio* calculations

The structure of phenol-N<sub>2</sub> in the electronic ground state has been optimized at the counterpoise gradient corrected HF and MP2/6-311G( $d,p$ ) level and at the CIS/6-311G( $d,p$ ) level for the electronically excited  $S_1$ -state with the GAUSSIAN 98 program package (Revision 11).<sup>28</sup> The SCF convergence criterion used throughout the calculations was an energy change below  $10^{-8}$  Hartree while the convergence criterion for the gradient optimization of the molecular geometry was  $\partial E/\partial r < 1.5 \cdot 10^{-5}$  Hartree/Bohr and  $\partial E/\partial \varphi < 1.5 \cdot 10^{-5}$  Hartree/deg, respectively. Additionally a

TABLE VI. Structural parameters of phenol-N<sub>2</sub>.

	$r_0$	pseudo- $r_s$	MP2 <sup>a</sup>	CAS(10/9) <sup>b</sup>
$S_0$	$R$ (pm)	233.1(3)	240.2	248.1
	$d_1$ (°)	158.2(58)	168.1	169.4
	$d_2$ (°)	208.5(195)	172.3	172.7
	$\chi^2$	2426	...	...
	$\sigma$	16.4	...	...
$S_1$	$R$ (pm)	220.8(21)	...	247.6
	$d_1$ (°)	157.9(60)	...	169.3
	$d_2$ (°)	200.8(195)	...	172.8
	$\chi^2$	2083	...	...
	$\sigma$	15.2	...	...
$\Delta R$ (pm)	-12.3	-14.5	...	-0.6

<sup>a</sup>Geometry optimized with the 6-311G( $d,p$ ) basis using counterpoise corrected gradients.

<sup>b</sup>Using the cc-pVDZ basis.

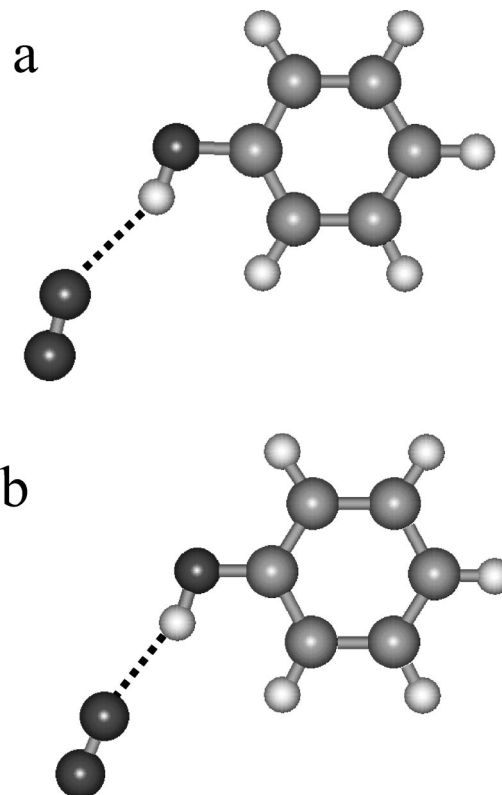


FIG. 4. (a) Pseudo- $r_s$ -structure of phenol-nitrogen in the electronic ground state. (b) Pseudo- $r_s$ -structure of phenol-nitrogen in the electronically excited state.

CASSCF calculation has been performed with ten electrons in nine orbitals. The active space is composed of the six aromatic  $\pi$ ,  $\pi^*$  orbitals located at the carbon atoms, the  $p_z$  lone pair orbital at the phenolic oxygen atom, and two orbitals from the nitrogen moiety (one occupied, one unoccupied) in the complex. The orbitals used in the resulting CAS(10/9) space are shown in Fig. 5.

The result of the above calculations along with a CAS(8/7) study, which contains only electrons localized at the phenol chromophore, from Watkins *et al.*<sup>9</sup> are given in Table VII.

The MP2 structure optimizations with the 6-311G( $d,p$ ) basis set reproduce the ground state rotational constants within 2% or better. It is necessary to apply counterpoise corrected gradients in the optimization, otherwise they converge to a different geometry largely deviating from the experimental one. The results of the latter calculations are given in parentheses in Table VII. The description of the cluster structure thus demands either a much larger basis set or the imperative use of counterpoise corrected gradients in the optimization.

The changes of rotational constants upon electronic excitation have been approximated by the difference between the rotational constants of a HF/6-311G( $d,p$ ) calculation for the ground state and a CIS/6-311G( $d,p$ ) calculation for the electronically excited state. The experimentally determined differences are reproduced with a surprising accuracy, which can be traced back to the similar deficiencies of both methods to describe the electron correlation. It can be concluded

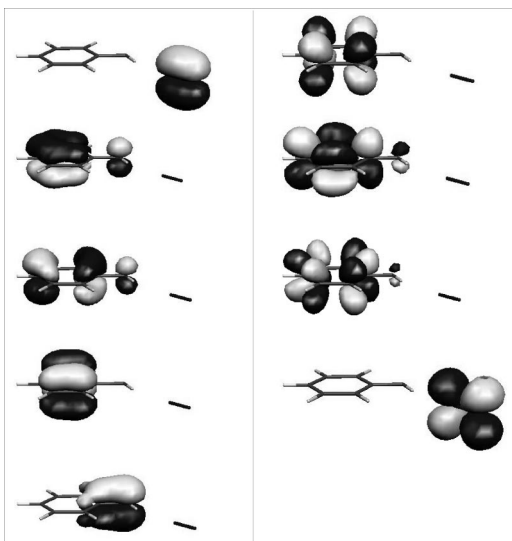


FIG. 5. The orbitals, which comprise the (10/9) space for the CASSCF calculations of phenol-nitrogen.

that the main interactions that stabilize the complex are multipole interactions, which can sufficiently well be described on the Hartree–Fock level.

An even better agreement between theory and experiment for both electronic states is found from the CAS(8/7)/cc-pVDZ calculations performed by Watkins *et al.*<sup>9</sup> The reported changes of the rotational constants upon electronic excitation as well as their absolute values in the  $S_1$ -state are in very good agreement with the experimental results.

Although the electronic excitation takes place mainly in the chromophore, we extended the active space in the calculations of the phenol-nitrogen complex to include two electrons in a  $\pi$ -orbital of the nitrogen moiety and the belonging  $\pi^*$ -orbital. The results for these CAS(10/9)/6-311G(*d,p*) and CAS(10/9)/cc-pVDZ calculations are presented in Table VII. Both calculations show a very good agreement with the experimentally determined rotational constants. The rota-

tional constants and geometries obtained from the CAS(10/9)/cc-pVDZ and the CAS(8/7)/cc-pVDZ are similar, but nevertheless show differences that might prove important if one tries to calculate molecular properties with “spectroscopic accuracy.”

Both  $r_0$  and pseudo- $r_s$  geometry predict a hydrogen bonded cluster as proposed by Ford *et al.*<sup>5</sup> For both structures the H $\cdots$ N distance is considerably shorter than predicted from the *ab initio* calculations and the nitrogen molecule deviates from a near linear hydrogen bond structure. One reason for this deviation might be zero-point vibrational effects on the geometry, which are contained in both  $r_0$  and pseudo- $r_s$  structure, but not in the  $r_e$  structure obtained from the *ab initio* calculations. Another explanation is the lack of electron correlation in the CASSCF calculations. This is supported by the fact that the MP2 calculations for the electronic ground state, which account for dispersion interactions, predict a shorter H $\cdots$ N distance than the CASSCF optimization of the ground state.

As can be inferred from Table VI, the decrease of the bond length upon electronic excitation is greatly underestimated at the CASSCF level. Theory predicts less than 1 pm decrease, while the experimentally determined reduction is found to be between 10 and 15 pm.

The angle  $\theta$  between the transition dipole moment (TDM) and the inertial  $a$ -axis was determined experimentally to be  $59.87^\circ$  for phenol-N<sub>2</sub> (cf. Table IV). This angle, determined at the CAS(10/9)/cc-pVDZ level of theory, is found to be  $57.08^\circ$  if the transition dipole moment in the cluster is assumed to be unchanged from that of the monomer. In the phenol monomer the TDM is found to be oriented along the inertial  $b$ -axis. Isotopic substitution rotates the inertial axes and changes therefore this angle. The experimentally determined value for  $\theta$  in  $d_1$ -phenol-N<sub>2</sub> is  $62.53^\circ$ , while the *ab initio* calculations give an angle of  $57.18^\circ$ . The increase of the angle  $\theta$  from theory is considerably smaller than determined experimentally. Thus in the CAS(10/9)/cc-pVDZ geometry the hydroxy group is located too close to the  $a$ -axis.

TABLE VII. Experimental and *ab initio* inertial constants of phenol-nitrogen. All calculations have been performed using the 6-311G(*d,p*) basis set.

	Expt.	MP2 <sup>a</sup>	HF	CIS	CIS-HF	CAS(8/7) <sup>b</sup>	CAS(10/9) <sup>c</sup>	CAS(10/9) <sup>d</sup>
$A''/\text{MHz}$	4072.18	4034(3858)	4197	...	...	4067.3	4155	4085
$B''/\text{MHz}$	648.01	635(679)	611	...	...	620.3	604	621
$C''/\text{MHz}$	559.26	548(578)	534	...	...	538.2	527	539
$A'/\text{MHz}$	3930.62	...	...	4102	...	3931.6	3997	3935
$B'/\text{MHz}$	663.72	...	...	622	...	615.9	600	617
$C'/\text{MHz}$	567.83	...	...	540	...	532.5	521	534
$\Delta A/\text{MHz}$	-141.56	...	...	...	-95	-135.7	-158	-150
$\Delta B/\text{MHz}$	15.71	...	...	...	11	-4.4	-4	-4
$\Delta C/\text{MHz}$	8.67	...	...	...	6	-5.7	-6	-5

<sup>a</sup>MP2 geometry optimization using counterpoise corrected gradients, the values in parentheses are optimized without counterpoise correction.

<sup>b</sup>From Ref. 9 using the cc-pVDZ basis.

<sup>c</sup>This study, using the 6-311G(*d,p*) basis set.

<sup>d</sup>This study, using the cc-pVDZ basis set.

#### IV. CONCLUSIONS

The structure of phenol-nitrogen has been determined in the electronic ground and first excited state to be planar hydrogen bonded. The rovibronic spectra of the electronic origins of four isotopomers could be measured and assigned with the aid of a genetic algorithm fit. This fit does not rely on prior assignments of quantum numbers to selected rovibronic transitions, which might be difficult in case of congested spectra. The fluorescence lifetime of phenol-N<sub>2</sub> and *d*<sub>5</sub>-phenol-N<sub>2</sub> was found to be 8 ns which is considerably longer than the lifetime of bare phenol (2 ns). Deuteration at the phenolic hydroxy group (*d*<sub>1</sub>-phenol-N<sub>2</sub> and *d*<sub>6</sub>-phenol-N<sub>2</sub>) increases the lifetime of the cluster to 17 and 14 ns, respectively. This is close to the value determined for bare *d*<sub>1</sub>-phenol (15 ns).

The intermolecular geometry, which was deduced from the inertial parameters to have an OH···NN pseudo-*r*<sub>s</sub> bond length of 225.5 pm (*r*<sub>0</sub>=233.1 pm), which is considerably shorter than the value obtained from a CAS(10/9)/cc-pVDZ calculation. This deviation can be traced back to a lack of electron correlation, which has to be included in the optimization of the cluster structure for both electronic states. CASPT2 calculations are currently on the way to improve the prediction of the geometry of the cluster in both electronic states.

#### ACKNOWLEDGMENT

The financial support of the Deutsche Forschungsgemeinschaft (SCHM 1043/9-4) is gratefully acknowledged. M.S. would like to thank the Nordrheinwestfälische Akademie der Wissenschaften for a grant which made this work possible.

- <sup>1</sup>Y. Hu, W. Lu, and S. Yang, *J. Chem. Phys.* **105**, 5305 (1996).
- <sup>2</sup>M. Schäfer and D. W. Pratt, *J. Chem. Phys.* **115**, 11147 (2001).
- <sup>3</sup>D. M. Chapman, S. R. Haines, W. D. Geppert, M. J. Watkins, K. Müller-Dethlefs, and J. B. Peel, *J. Chem. Phys.* **111**, 1955 (1999).
- <sup>4</sup>S. R. Haines, W. D. Geppert, D. M. Chapman, M. J. Watkins, C. E. H. Dessent, M. C. R. Cockett, and K. Müller-Dethlefs, *J. Chem. Phys.* **109**, 9244 (1998).
- <sup>5</sup>M. S. Ford, S. R. Haines, I. Pugliesi, C. E. H. Dessent, and K. Müller-Dethlefs, *J. Electron Spectrosc. Relat. Phenom.* **112**, 231 (2000).
- <sup>6</sup>A. Fujii, M. Miyazaki, T. Ebata, and N. Mikami, *J. Chem. Phys.* **110**, 11125 (1999).
- <sup>7</sup>T. Watanabe, T. Ebata, S. Tanabe, and N. Mikami, *J. Chem. Phys.* **105**, 408 (1996).
- <sup>8</sup>H. Watanabe and S. Iwata, *J. Chem. Phys.* **105**, 420 (1996).
- <sup>9</sup>M. J. Watkins, K. Müller-Dethlefs, and M. C. R. Cockett, *Phys. Chem. Chem. Phys.* **2**, 5528 (2000).
- <sup>10</sup>N. Solca and O. Dopfer, *Chem. Phys. Lett.* **325**, 354 (2000).
- <sup>11</sup>M. Schmitt, J. Küpper, D. Spangenberg, and A. Westphal, *Chem. Phys.* **254**, 349 (2000).
- <sup>12</sup>M. Okrusch, R. Müller, and A. Hese, *J. Mol. Spectrosc.* **193**, 293 (1999).
- <sup>13</sup>R. D. Suenram, F. J. Lovas, and G. T. Fraser, *J. Mol. Spectrosc.* **127**, 472 (1988).
- <sup>14</sup>W. Caminati and S. di Bernardo, *J. Mol. Struct.* **240**, 253 (1990).
- <sup>15</sup>S. Gerstenkorn and P. Luc, *Atlas du Spectre d'Absorption de la Molécule d'Iode* (CNRS, Paris, 1982).
- <sup>16</sup>J. A. Hageman, R. Wehrens, R. de Gelder, W. L. Meerts, and L. M. C. Buydens, *J. Chem. Phys.* **113**, 7955 (2000).
- <sup>17</sup>W. L. Meerts, M. Schmitt, and G. Groenenboom, *Can. J. Chem.* (submitted).
- <sup>18</sup>Y. R. Wu and D. H. Levy, *J. Chem. Phys.* **91**, 5278 (1989).
- <sup>19</sup>A. L. Sobolewski and W. Domcke, *J. Phys. Chem. A* **105**, 9275 (2001).
- <sup>20</sup>R. J. Lipert and S. D. Colson, *J. Phys. Chem.* **93**, 135 (1989).
- <sup>21</sup>A. Sur and P. M. Johnson, *J. Chem. Phys.* **84**, 1206 (1986).
- <sup>22</sup>C. Ratzer, J. Küpper, D. Spangenberg, and M. Schmitt, *Chem. Phys.* **283**, 153 (2002).
- <sup>23</sup>K. Levenberg, *Q. Appl. Math.* **2**, 164 (1944).
- <sup>24</sup>D. D. Marquardt, *J. Soc. Ind. Appl. Math.* **11**, 431 (1963).
- <sup>25</sup>N. W. Larsen, *J. Mol. Struct.* **51**, 175 (1979).
- <sup>26</sup>J. Berndtsen, *J. Raman Spectrosc.* **32**, 989 (2001).
- <sup>27</sup>C. Costain, *J. Chem. Phys.* **29**, 864 (1958).
- <sup>28</sup>M. J. Frisch, G. W. Trucks, H. B. Schlegel *et al.*, GAUSSIAN 98, Revision A.11, Gaussian, Inc., Pittsburgh, PA, 2001.